이학석사 학위논문

Evaluation of histopathological changes of vasculature in recurrent chronic subdural hematoma

재발한 만성 경막하 혈종에서 혈관 구조 변화의
조직 병리학적 평가

2021 년 08 월

서울대학교 융합과학기술대학원
분자의학 및 바이오제약학과

김 현

재발한 만성 경막하 혈종에서 혈관 구조 변화의 조직 병리학적 평가

Evaluation of histopathological changes of vasculature in recurrent chronic subdural hematoma

지도교수 이 동 수

이 논문을 김 현 석사 학위논문으로 제출함

2021년 7월

서울대학교 융합과학기술대학원

분자의학 및 바이오제약학과

김 현

김 현의 이학석사 학위논문을 인준함

2021년 7월

위 원 장 신 영 기

부 위 원 장 이 동 수

위 원 서 민 석

Abstract

Evaluation of histopathological changes of vasculature in recurrent chronic subdural hematoma

Hyun Kim

Molecular Medicine and Biopharmaceutical Sciences

WCU Graduate School of Convergence Science and Technology

Seoul National University

Chronic subdural hematoma (cSDH) is a collection of blood in subdural space with encapsulated hematoma by neomembrane. The incidence of cSDH is increasing, especially in the aging population. Although hematoma is removed by surgical interventions, a considerable percentage of patients undergo recurrence. Still, the underlying mechanism of spontaneous recurrence has not been unveiled and there is no standard management. To figure out the unsolved issues of spontaneous recurrent cSDH, I observed histopathology of cSDH dura mater, focusing on the vasculature changes.

Control dura and cSDH dura were harvested from patients and compared to each other. The immuno-staining technique was mainly used to visualize the vasculatures. The dura tissues were cleared transparently by CLARITY to observe 3-dimensional structure in the whole dura layers. Additionally, transmission electron microscopy (TEM) was used for observing capillaries and their endothelial cells.

As a result, meningeal dura in cSDH was thinner than control. In contrast, the dural border cell (DBC) layer was thicker as it turned into neomembrane. In the cSDH neomembrane, vascular volume density was 5.9 times higher than the DBC layer of control dura mater. The sinusoidal capillaries were found in the neomembrane by taking TEM images. Also, the volume density of arteries in the neomembrane was 5.4 times higher than the control DBC layer. These arteries in the neomembrane were connected to the middle meningeal artery (MMA). In addition, changes in lymphatic vessel morphology were observed such as the formation of sprouts and loops. 26.9 times more sprouts and 58.8 times more loops were formed per volume than control.

Accordingly, increased vessel density and formation of fragile and leaky capillaries in the neomembrane layer were observed, which suggest neovascularization in the cSDH dura. Especially, the connection between MMA and dense arteries in the neomembrane of cSDH dura was visualized. These results may support the hypothesis of spontaneous recurrent cSDH and the therapeutic effect of MMA embolization.

Keywords: chronic subdural hematoma, dura mater, neomembrane, sinusoidal capillary, middle meningeal artery, neovascularization, lymphangiogenesis

Student Number: 2019-28947

Table of Contents

Introduction

Chronic subdural hematoma (cSDH) is an accumulation of blood covered with neomembrane in subdural space. The incidence of cSDH has increased twice from 8.2 to 17.6 per 100,000 persons per year from 1990-2015. Especially, the ≥80-year-old people showed about 6 times higher cSDH incidence rate than younger adults[1,2]. Moreover, 2 to 37 percentage of cSDH patients undergo recurrence of bleeding even after surgical interventions[1,2,3]. For figure out the reason of spontaneous recurrence and find a novel treatment for cSDH, it is important to understand the underlying characteristics of recurrent cSDH.

The human brain is covered by a membrane called the meninges. Meninges consists of multilayer as dura, arachnoid, and pia mater. Dura mater is the hardest one and it is divided into three layers. Periosteal dura attaches to the skull and includes large vessels like the middle meningeal artery (MMA). Meningeal dura is under the periosteal dura and it contains lesser collagen and denser cells than periosteal dura. In last, the dural border cell (DBC) layer is on the bottom of these two layers, and it is the thinnest and contains loose fibrous tissues. This layer turns into the neomembrane and encapsulates the hematoma in cSDH. A space between the DBC layer and arachnoid mater is called subdural space[4] (Figure.1).

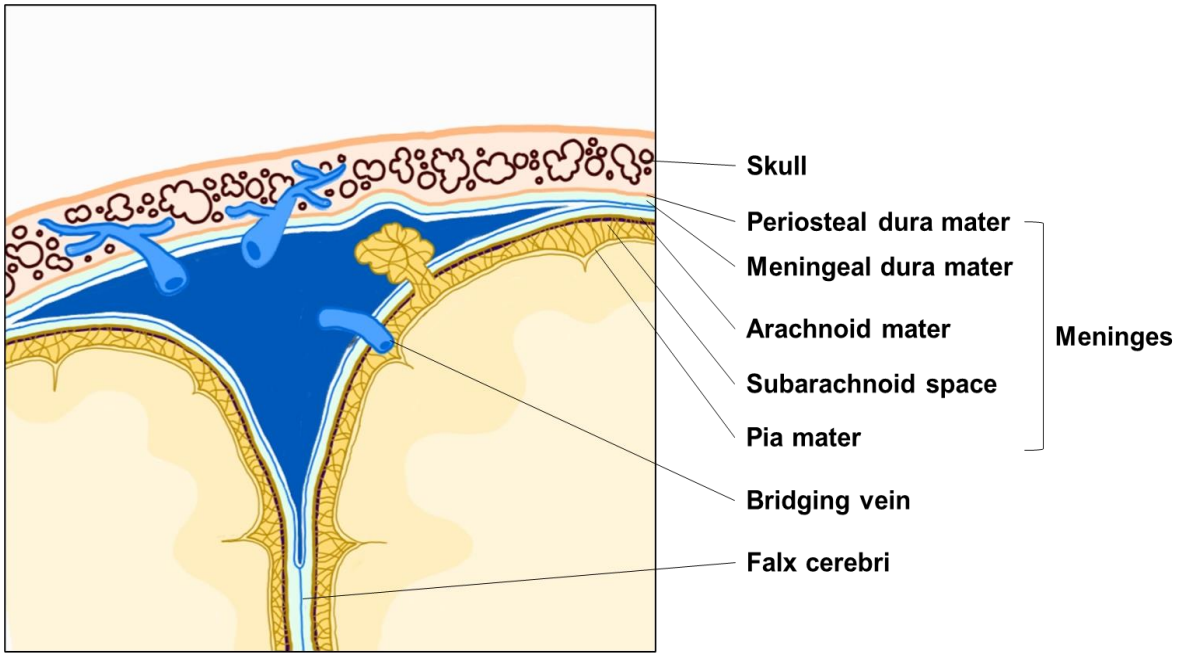

Figure 1. Human brain and meninges structures.

Illustration of the human brain and meninges. Meninges covers brain and it consists of three layers, dura, arachnoid, and pia mater. Bridging veins are veins in the subarachnoid space which puncture the dura mater and dural venous sinuses.

The main risk factor of SDH is trauma. Trauma evokes tearing of bridging veins, and cortical vessels, separation of the dura-arachnoid junction, and rupture of arterial twig[5,6]. These damages lead to the formation of SDH, and hematoma is slowly developed over the 3 weeks in case of cSDH.

About 80% of cSDH patients without mass effect showed spontaneous regression of hematoma without any treatments[10]. Some cSDH patients were treated by medications such as steroids, angiotensin-converting-enzyme inhibitors, and platelet-activating factor receptor antagonist[11,12,13]. The other cSDH patients with mass effect need surgical removals like small burr hole trephination, craniotomy, and SDH evacuation[1,3,5,14]. In spite of these conventional surgical removals, the cSDH recurrs[1,2,3]. Some reasons of recurrent cSDH are definite such as trauma, drugs, and medical disease but, the mechanism of spontaneous recurrent cSDH remains still unclear. The main hypothesis is that fragile new vessels from the neomembrane are repeatedly ruptured and micro-hemorrhage enlarges to hematoma[1,2,4,5,17]. In addition, MMA might be related to the reason of spontaneous recurrent cSDH. Because MMA embolization which was introduced as a novel treatment for cSDH recently showed relatively lower recurrence rate of cSDH than conventional surgical removals (1.4% vs. 27.5%)[15,30].

To figure out the cause of spontaneous recurrent cSDH and contribute to finding standard management, the histopathological changes in cSDH dura were observed by comparing to control. The control dura sample was isolated from subarachnoid hemorrhage (SAH) patient and the dura with cSDH was harvested from cSDH patient. Morphological, and structural changes of vasculature in the dura were comprehensively evaluated.

Materials and Methods

Sampling of the dural specimen

Human dura samples of dura mater were acquired under the approval of the institutional review board. Control dura mater was sampled from a 54-year-old female patient who was diagnosed SAH undergoing surgical clipping of unruptured intracranial aneurysm, who have never been operated on. A dura mater with cSDH was harvested in a 56-year-old male patient who underwent fronto-temporal craniotomy, clipping of unruptured aneurysm in the anterior communicating artery, and evacuation of the cSDH. One month ago, the patient underwent a left-sided craniotomy and SDH evacuation of multilayered cSDH (Figure.2a). The patient had a history of minor head trauma a few months ago, with no other medical problems.

Intraoperatively, SDH was covered with neomembrane and detached with a few membranes, in which outer neomembrane was attached to the inner dura mater and was slightly thick; meanwhile, the inner neomembrane was less firmly attached to the arachnoid mater and was thinner than the outer neomembrane. Outer neomembrane contents included dark brownish fluid and hard old clot. When the outer neomembrane was peeled from the dura mater, fine blood oozing from the inner dural surface was observed at that area. However, there was no bleeding in the inner neomembrane from the arachnoid mater. Dura mater tissues were too large to experiment, so control dura, and cSDH dura with the outer neomembrane were resected in a small size (Figure.2b).

a.

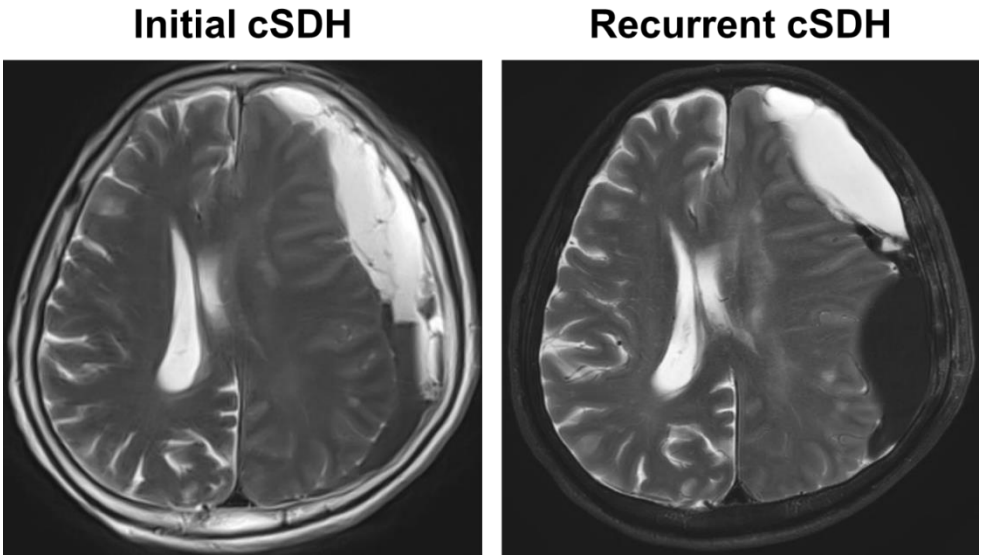

b.

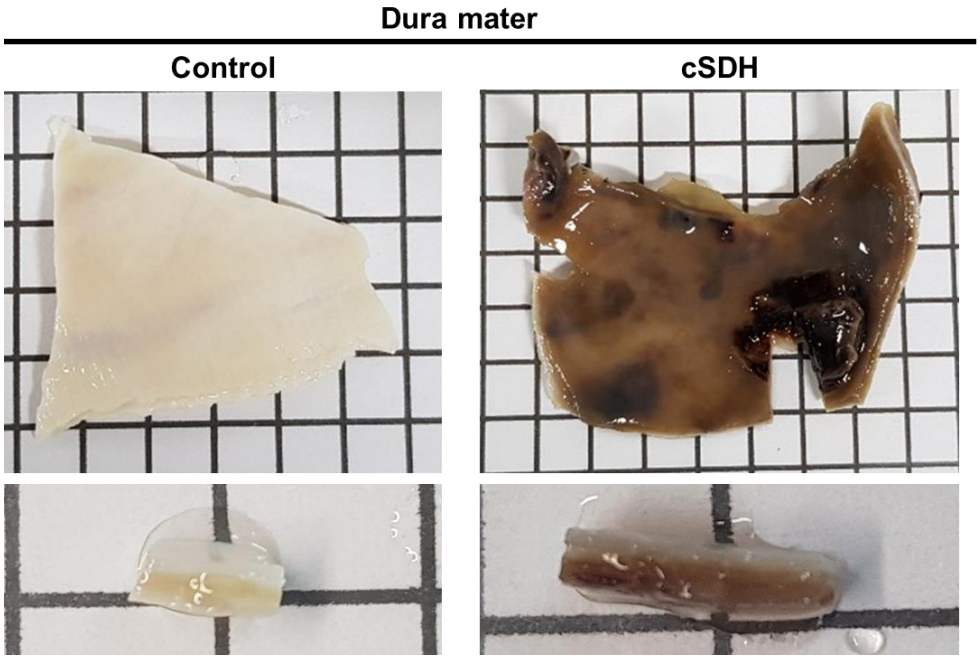

Figure 2. cSDH patient characteristics and dura samples.

a. A 56-year-old male presented with an cSDH. Initial brain MR reveals a multilayered cSDH on the left side. After the patient underwent SDH evacuation, cSDH recurred spontaneously on the same side.

b. Gross photos of the harvested the control dura and the cSDH dura including outer neomembrane.

Tissue clearing

To observe various types of vessels and their structures 3 dimensionally, clear lipidexchanged acrylamide-hybridized rigid imaging-compatible tissue-hydrogel (CLARITY) tissue clearing technique was performed in dura tissues. Dura samples were fixed in 10% formalin after isolation and stored at 4℃ at least 24hrs. The samples were cut into smaller pieces and put in a 40% acrylamide solution for scaffolding. After 1 day of incubation at 4℃, filled nitrogen gas in the bottles and incubated at 37℃ for 5hrs in the dark. These polymerization stages support tissue structures even after lipids were cleared through electrophoresis. Since non-sliced tissues are too thick to penetrate, tissues were incubated in DeepLabel™ Solution A (Logos Biosystem, #C33002) to increase permeability. Then, the tissues were incubated in DeepLabel™ Solution B (Logos Biosystem, #C33003) with primary antibodies at 37℃. After 7 days of incubation, the dura samples were washed by phosphate-buffered saline (PBS) with tween 20 and incubated for 5 days with secondary antibodies. After the incubation samples were washed using PBS with tween 20, samples were incubated in X-CLARITY™ Mounting Solution (Logos Biosystem, #C13101) overnight at 37℃. Going through a series of processes, the refractive index (R.I) of tissue changes, the tissue finally became transparent. Using Leica confocal microscopy SP8, took images from those stained samples. (Figure.3)

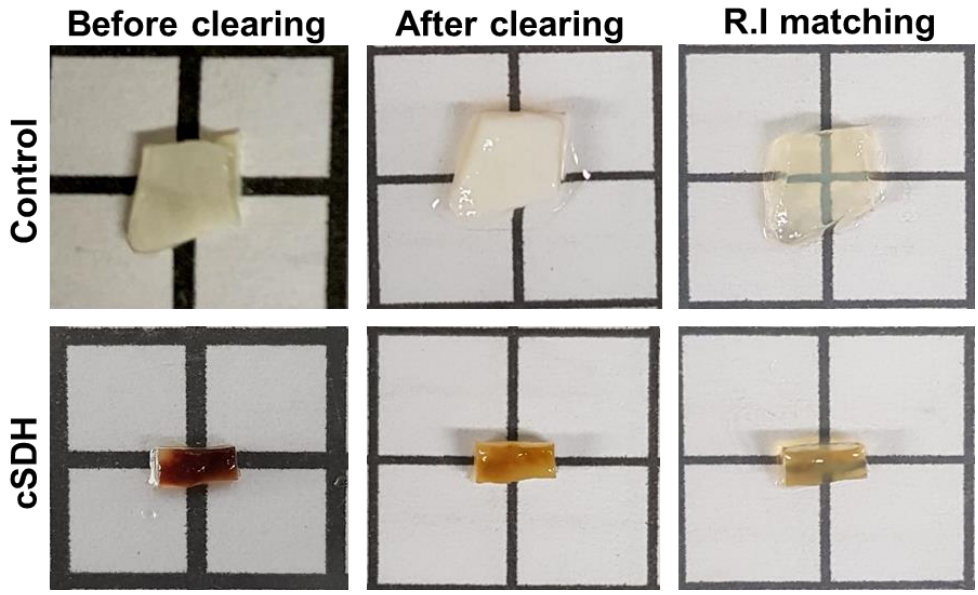

Figure 3. Stages of tissue clearing.

Image of tissue clearing stages. Before clearing images show gross photos of the control dura and the cSDH dura. After clearing images indicate depletion of lipid in tissue with polymerization. Refractive index (R.I) of tissue changes after treated mounting solution. After matching R.I, the tissue becomes completely transparent.

Immunohistochemistry

Selected regions in the dura samples were embedded in paraffin and analyzed with 4μm sections. These sectioned samples were deparaffinized in xylene and rehydrated serially in 100-70% ethanol solutions. In the antigen retrieval step, the tissue was boiled in the solution made by citric acid and tri-sodium citrate for 10min. To increase the permeability, tissues were incubated in the 0.5% TritonX-100 in PBS and the slides were incubated again for 60min in the 5% bovine serum albumin in PBS to block non-specific antigens. Then, tissue slides were incubated overnight with primary antibodies against laminin (Sigma Aldrich, #L9393), α smooth muscle actin (αSMA) (Abcam, #ab7817), lymphatic vessel endothelial hyaluronan receptor-1(LYVE-1) (Abcam, #ab14917), Podoplanin (PDPN) (Abcam, #ab77854) at 4℃. Laminin is a marker of basement membrane which covers outside of the vessels, and αSMA shows mural cells and pericyte on vessels. LYVE-1 and PDPN are markers of lymphatic endothelial cells. After incubation, slides were washed with PBS and incubated for 1hr with secondary antibodies in room temperature. The samples were washed again and mounted using VECTASHEILD® mounting solution (Vector Laboratories, #H-1000). To capture stained images, Leica confocal microscopy SP8 was used.

Measurement of vessel and tissue volume

To measure the volume of whole tissues and stained vasculatures, IMARIS (Oxford instrument) was used. This image analysis software merged and reconstructed taken images from Leica confocal microscopy SP8. After forming 3-dimensional images, the surface analysis technique in IMARIS technically targets the fluorescent regions and measured their surfaces and volumes. Using this function, 3 pieces of control dura and 3 pieces of cSDH dura were used for

measuring vascular volume. Also, another 3 pieces of control dura and 3 pieces of cSDH dura were used for measuring artery volume.

Transmission Electron Microscopy (TEM)

TEM (JEOL, JEM-1400) images were taken at Seoul National University, Korea. The dura samples were fixed in 10% formalin and washed in PBS overnight. Then, samples were washed in Sorenon's phosphate buffer and fixed 2% osmium tetroxide. After dehydrated in alcohol, propylene was treated and embedded in Spurr's embedding media. Ultrathin sectioned samples were mounted on copper grids and stained with uranyl acetate and lead citrate.

Results

Part 1. Morphologic change of dura in cSDH

In the periosteal layer, large blood vessels like MMA and numerous vertical lines were found but no difference between the control and cSDH dura samples. However, the meningeal and DBC layer in cSDH showed different morphologies compared to control. The meningeal layer was thinner and slightly denser in cSDH. In contrast, the neomembrane layer in cSDH was thicker and had looser connective tissues than the DBC layer in control. Also, relatively large voids and erythrocytes between tissues were found in this layer. Below the neomembrane, I additionally observed the large amounts of erythrocytes presumed to be hematoma with ambiguous border. (Figure. 4)

a.

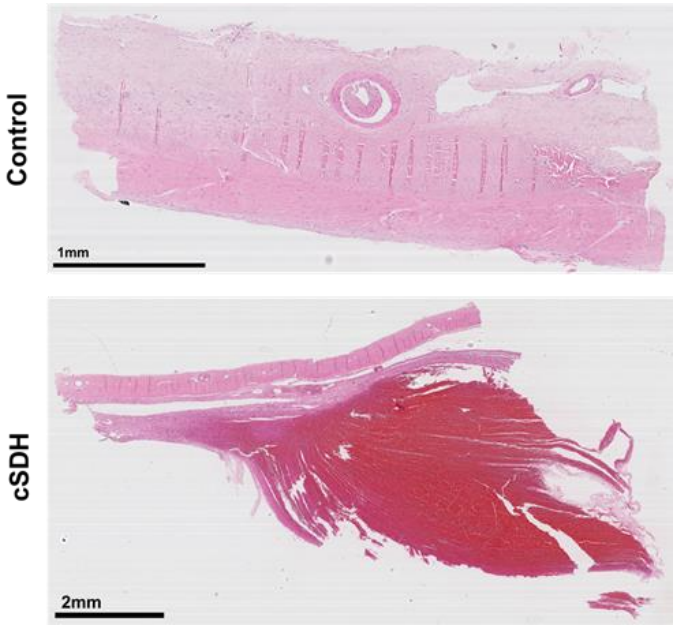
Control
1mm
cSDH
2mm

b.

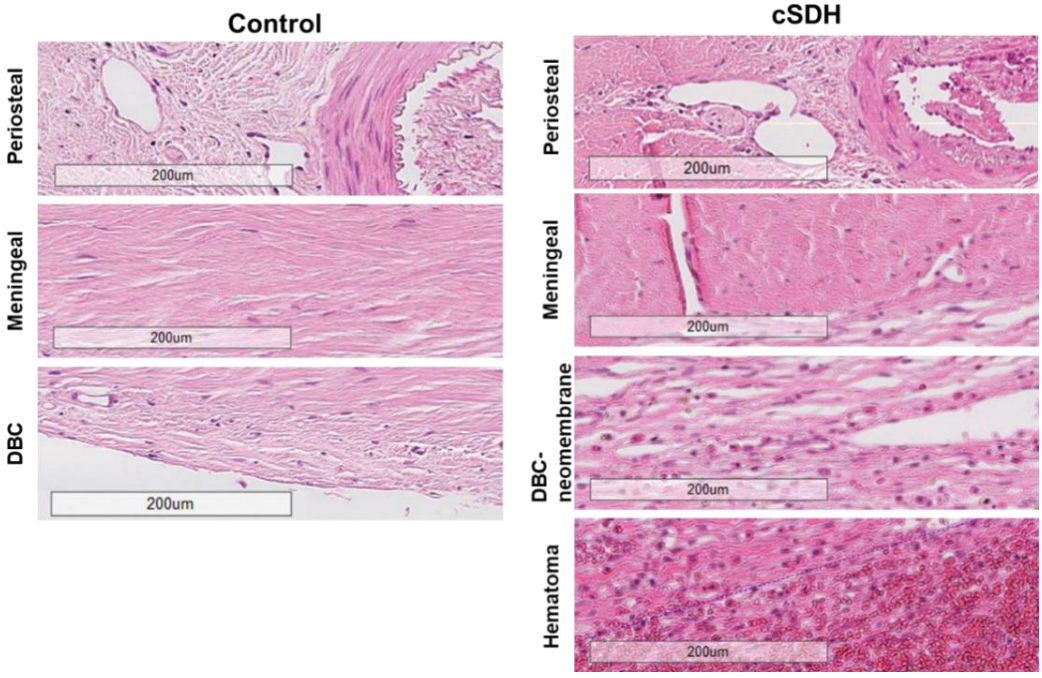
Control
cSDH
Periosteal
Meningeal
DBC
DBC-neomembrane
Hematoma
200um

c.

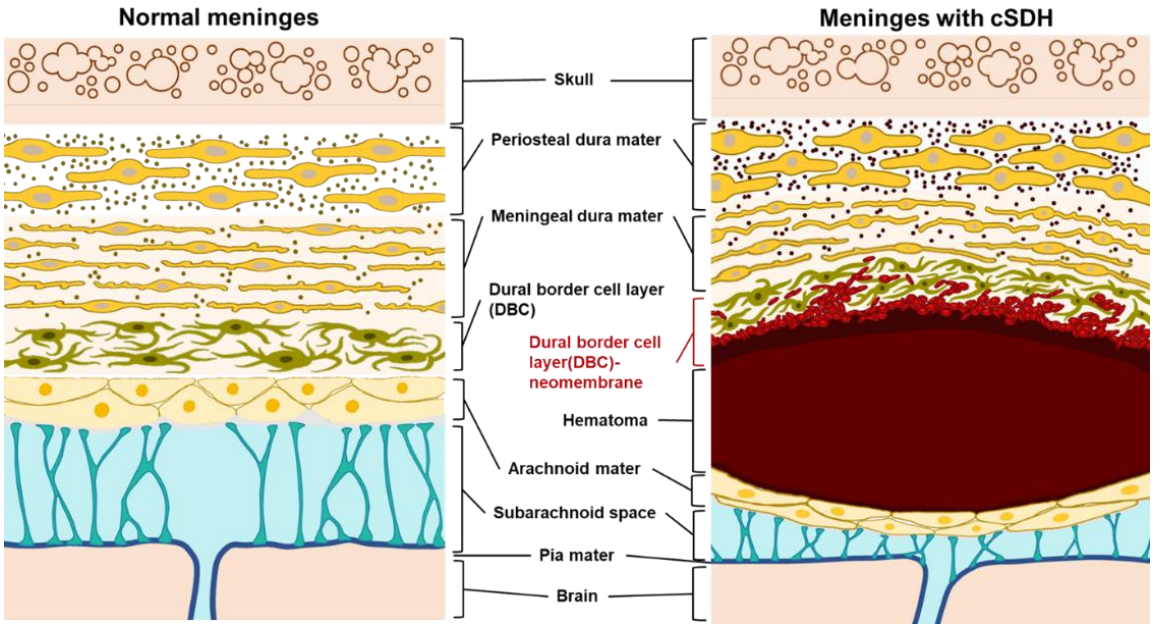

Figure 4. Morphological characteristics in control and cSDH dura.

a. H&E staining of the control and the cSDH patient whole dura layer. Dura with cSDH tissue included neomembrane and hematoma.

b. Enlarged each layer of the dura and divided them. Compared to the DBC layer in control, the neomembrane shows much looser connective tissues and numerous voids. The blue-dash line in the hematoma layer is the boundary between the neomembrane and hematoma.

c. The illustration shows the characteristics of each layer in meninges. Subdural hematoma presses all layers of meninges and it forms a neomembrane by changing the DBC morphology.

Part 2. Vasculature changes in cSDH dura

Vascular density in neomembrane of cSDH dura

To observe vasculature in the dura, laminin and αSMA were targeted for immunostaining. Laminin is a marker of the basement membrane which is contained all vascular structures not only blood vessels but also, lymphatic vessels. αSMA staining usually indicates mural cells and pericytes covering the vessels which are mostly in smooth muscle cells on arteries.

Results of IHC showed that the number of vessels in the neomembrane of cSDH had more than the DBC layer in control. The number of vessels per area(mm^2) of control was 20.7 and cSDH was 78.9 on average. This calculation proved that 3.8 times more vessels per area(mm^2) were in the cSDH neomembrane than the control DBC layer. (Figure. 5)

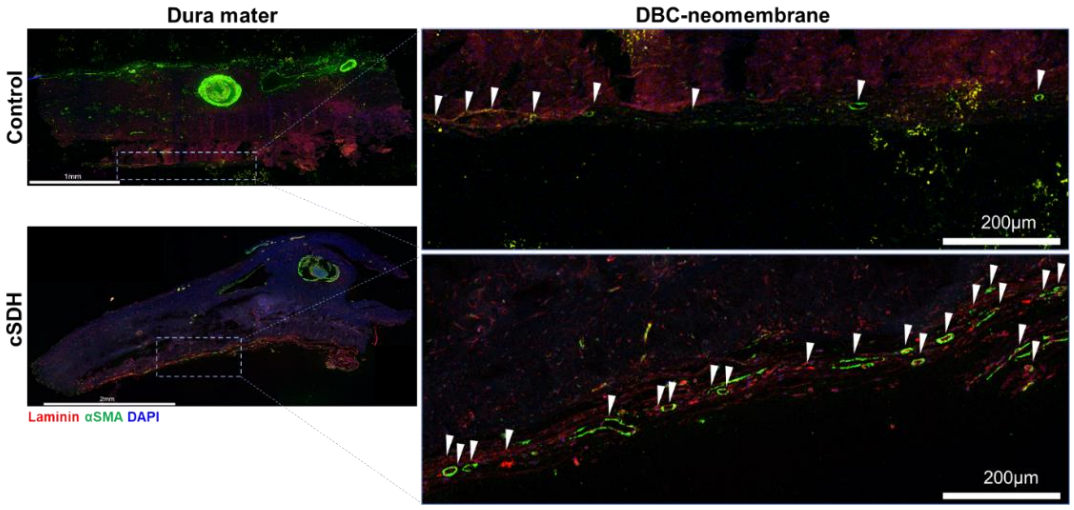

Figure 5. The number of vessels per area in the control DBC layer and the cSDH neomembrane.

IHC results show the vessels in the control DBC layer and the cSDH neomembrane. Left dura mater figures are overlay image of DAPI(blue), laminin(red), and αSMA(green). Scale bar 1mm for control image. Scale bar 2mm for cSDH image. DBC-neomembrane figures are enlarged images derived from left whole dura layer images. Scale bar 200μm. White arrows point to each vessel. Compared to the same layer of the tissues, the number of white arrows in the neomembrane was higher than the control.

Also, laminin staining was performed with tissue clearing and I analyzed vessel volume density per DBC layer of control and neomembrane layer of cSDH volume(μm^3). Magnified vessel area directly showed that cSDH neomembrane contained more vessel structures than control DBC layer. As a result of calculating volume, the vessel volume per tissue volume(μm^3) in the cSDH neomembrane layer was 5.9 times higher than the DBC layer in control. These results may indicate the neovascularization in the cSDH neomembrane. (Figure. 6)

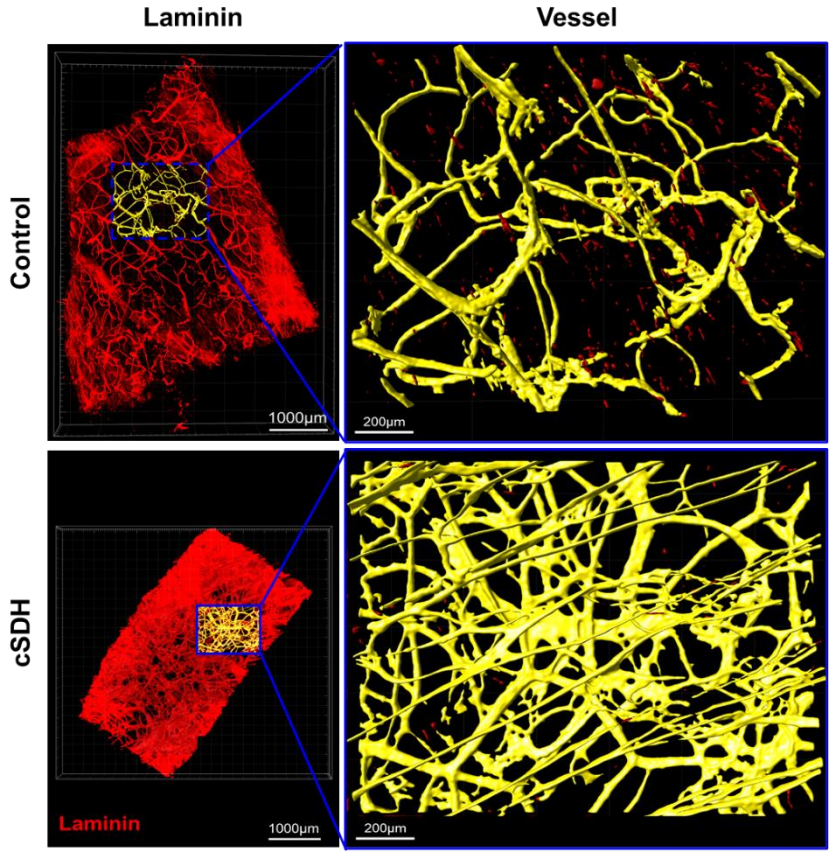

Figure 6. Visualization of laminin-positive vasculature in the DBC layer of control and the neomembrane of cSDH dura.

3-dimensional images of vasculatures in the control DBC layer and the cSDH neomembrane stained by laminin(red). Scale bar 1000μm. Yellow vessels show part of the same volume in each tissue and magnified. Scale bar 200μm. Denser vessels were found in cSDH than control. The whole area of the tissues was measured in its vascular volume (μm^3).

Capillary structures in neomembrane of cSDH dura

To confirm the reports of sinusoidal capillaries in the neomembrane of cSDH, features of capillary were observed by taking TEM in the control DBC layer and the cSDH neomembrane. Capillary consists of one layer of endothelial cells connected with junctions and adhesion molecules. I found capillaries surrounded by endothelial cells with tight junctions like continuous capillary in both dura. Additionally, different two more capillaries were discovered in the neomembrane of cSDH but not in the control DBC layer. One of them showed a pore with diaphragm between endothelial cells like fenestrated capillary. The other one had gaps without any junctions or diaphragms between endothelial cells like sinusoidal capillary. (Figure. 7)

a.

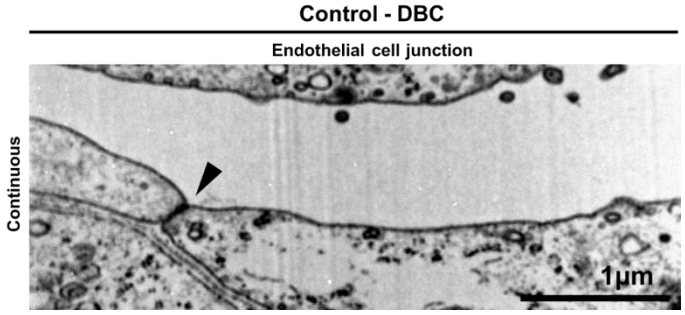
Control - DBC
Endothelial cell junction
Continuous
1µm

b.

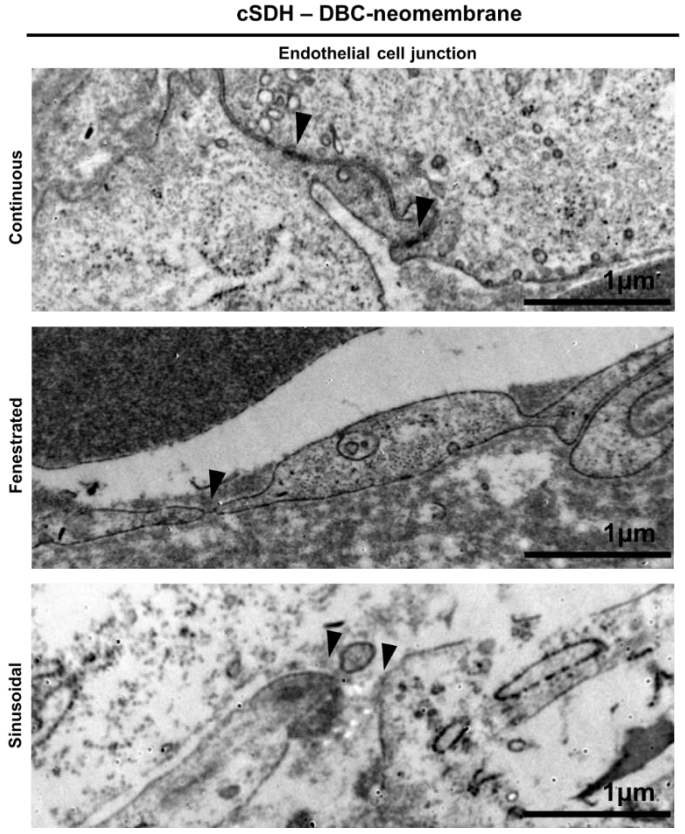
cSDH – DBC-neomembrane
Endothelial cell junction
Continuous
1µm
Fenestrated
1µm
Sinusoidal
1µm

Figure 7. Type of capillaries in the DBC layer of control and the neomembrane of cSDH dura.

TEM images of capillaries in the control DBC layer and the cSDH neomembrane.

a. Continuous capillaries were only observed in the control DBC layer. Black arrow indicates a tight junction between the endothelial cells. Scale bar 1μm.

b. Continuous, fenestrated capillary, and sinusoidal capillary were found in the neomembrane. Black arrows in the continuous capillary point the tight junctions. A black arrow in fenestrated capillary points a pore with diaphragm. In sinusoidal capillary, black arrows indicate gaps with no junctions and diaphragms. Scale bar 1μm.

Arterial vasculature in cSDH dura

The whole dura layer was stained with αSMA including periosteal and meningeal layers to observe the whole structure of the artery in the dura. Relatively large-scaled arteries in the periosteal layer were MMA. The MMA branched out arteries called penetrating artery and they connected to small arteries in the DBC layer. In cSDH dura, the MMA was connected to abundant arteries in the neomembrane through penetrating arteries. Arteries in the cSDH neomembrane widely distributed and looked denser than arteries in the control DBC layer. (Figure.8a)

Since the previous results, I compared artery volume density in the control DBC layer and the cSDH neomembrane. The neomembrane contained 5.4 times higher artery volume density rather than the control DBC layer on average. It indicates that the artery also may be neovascularized in the neomembrane. (Figure.8b)

a.

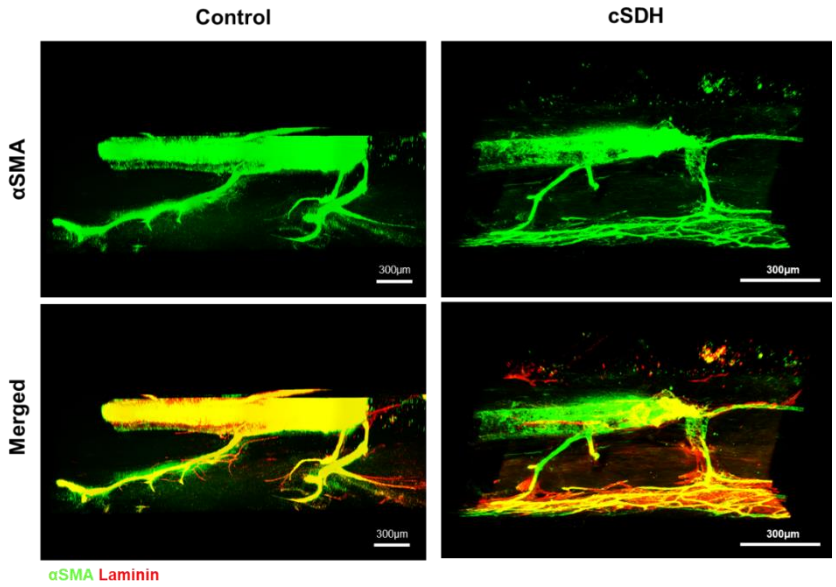
Control
cSDH
αSMA
Merged
300μm
300μm
300μm
300μm
αSMA Laminin

b.

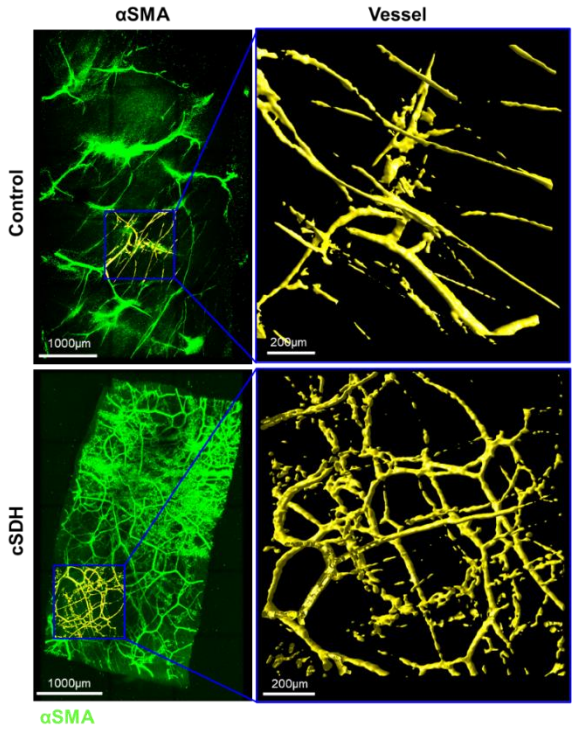
αSMA
Vessel
Control
cSDH
1000μm
200μm
1000μm
200μm
αSMA

Figure 8. Arterial vasculatures in the control and cSDH dura.

a. To visualize the artery, αSMA(green) was used in immunostaining. There are the connections between MMA and arteries in the DBC layer of control or the neomembrane of cSDH dura. Especially, the arteries in the neomembrane of cSDH were widely distributed and looked denser. Scale bar 300μm.

b. Visualization of arteries in the DBC layer and the neomembrane**.** Scale bar 1000μm. Yellow vessels show part of the same volume in each tissue and magnified. Scale bar 200μm. Denser arteries were observed in the cSDH than the control.

Lymphatic structure in cSDH dura.

To selectively stain lymphatic vessels, LYVE-1, PDPN, and laminin antibodies were used for immunostaining. LYVE-1 exists on the lymphatic endothelial cell surface and PDPN is a protein that has been found in lymphatic endothelial cells either[17]. So, those two markers have been used for targeting lymphatic endothelial cells.

Compared to control, different lymphatic vasculatures were found in cSDH dura, especially near large vessels in the periosteal layer. I observed that the sprout and loop structures of lymphatic vessels in cSDH dura. These structures also could be found in control but much less than cSDH. Four-part of dura tissues in each sample were stained and counted the number of sprouts and loops per tissue volume(μm^3). As a result, the number of sprouts per volume(μm^3) in cSDH was 26.9 times higher than control on average. Also, the number of loops per volume(μm^3) in cSDH was 58.8 times more than control. These results imply that lymphangiogenesis occurred in the cSDH condition. (Figure.9)

a.

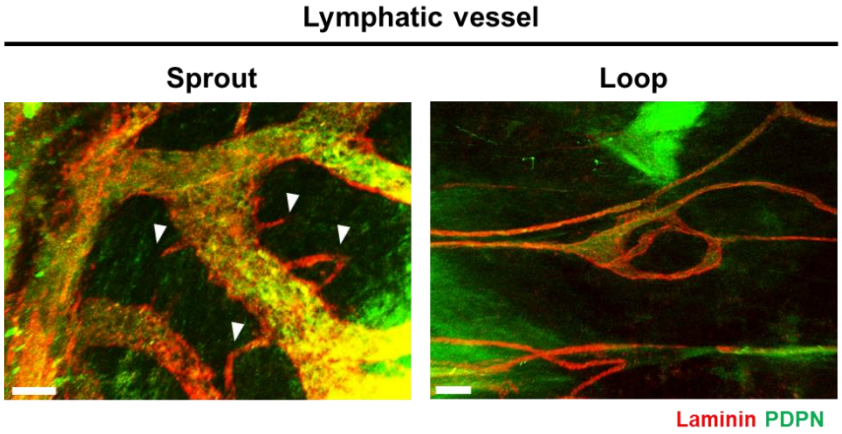

b.

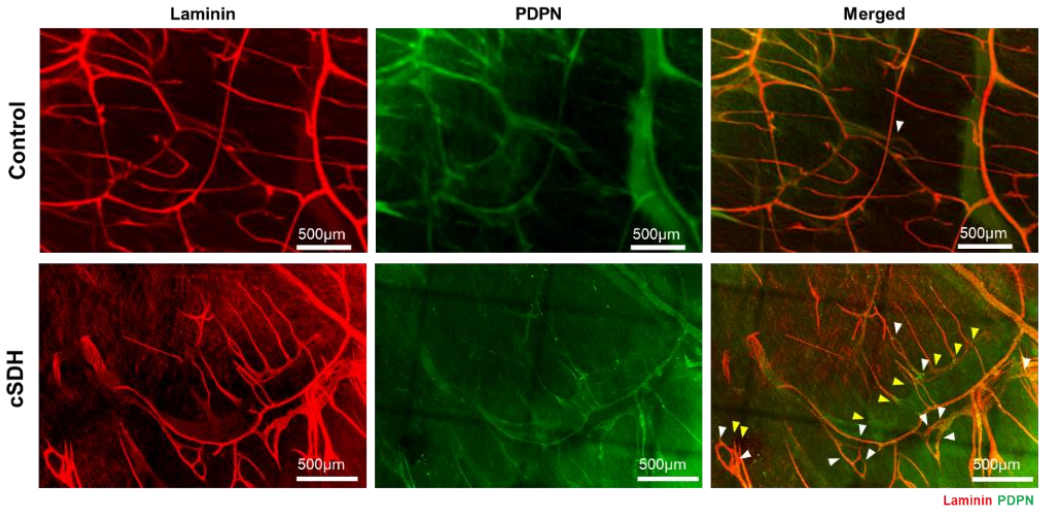

Figure 9. Lymphatic vasculatures in control and cSDH dura.

Lymphatic vasculatures were visualized in both dura tissues.

a. Lymphatic sprout and loop structures were observed in the cSDH dura. White arrows indicate the sprouts from existing lymphatic vessels.

b. Compared to the control dura, the number of sprouts and loops were higher in the cSDH dura. Yellow arrows point sprouts and white arrows point loops. Scale bar 500μm.

Discussion

cSDH condition induces changes in the layer morphologies and vasculatures including lymphatic vessels. The meningeal layer was thinner but, the DBC layer was dramatically thicker than the control. In the neomembrane layer, the density of vessels was higher than the control DBC layer. The sinusoidal capillaries were found in the neomembrane and the density of arteries also higher than the control DBC layer. Moreover, I observed the connections between arteries in the neomembrane and MMA in the periosteal layer. Also, more lymphatic sprouts and loops were found in the cSDH which have been considered evidence of lymphangiogenesis.

Compared to the control, the meningeal dura was thinner, and the DBC layer was thicker in the cSDH dura. The thinner meningeal layer in the cSDH dura could happen by the pressure of hematoma or, maybe because the thickness of the dura layer can be different depending on the individual. The reason for the thicker DBC layer in cSDH is the formation of neomembrane. The accumulated blood between the dura and arachnoid mater damages the DBC layer. It recruits inflammatory cells that attempt to repair the delaminated DBC layer by forming granulation tissue. Also, blood and cSDH fluid contain high concentration of type 1 (PICP) and type 3 (PIIINP) procollagen and those factors induce proliferation of DBCs to fibrous connective tissue. Then, the collagen matrix is continuously formed as a repair process. Moreover, eosinophils express transforming growth factor (TGF-β1) and induce SMAD signaling. This SMAD signaling pathway persists in fibrosis which contributes to developing the neomembrane. Therefore, the creation of collagen matrix and proliferation of DBCs formed the neomembrane layer, which is inevitably thicker than control DBC layer. For these reasons, I considered that the DBC layer in the control dura sample and the neomembrane layer in the cSDH dura sample were the same layers.

The number of vessels per area (mm^2) and volume density of vessels per tissue volume (μm^3) in the cSDH neomembrane were higher than the control DBC layer. These results indicate the occurrence of neovascularization in the neomembrane layer.

Neovascularization is induced by inflammation from hematoma. The accumulation of blood recruits inflammatory cells such as lymphocytes, neutrophils, macrophages, and eosinophils, and those cells migrate to the bleeding region. Inflammatory cells release pro-inflammatory cytokines (IL-1, -2R, -5, -6, -8, -17) and anti-inflammatory cytokines (IL-10, 13). Angiopoietin-2 (Ang-2) and vascular endothelial growth factors (VEGFs) are representative pro-angiogenic factors that are overexpressed in cSDH neomembrane[17-20]. The level of VEGF and vascular endothelial growth factor receptor (VEGFR) is significantly higher in cSDH fluid compared with peripheral blood and cerebrospinal fluid (CSF). In addition, cSDH fluid contains a high concentration of prostaglandin E (PGE2) and hypoxia-inducible factor 1α (HIF-1α). Those factors regulate VEGF expression[18,19]. In particular, vascular regeneration in meninges after a head injury is managed by VEGFR2 signaling. VEGF-A predominantly binds to VEGFR2 and this VEGF-A/VEGFR2 signaling increases Dll4-Notch signaling in tip endothelial cells[21]. Highly contained angiogenic factors and inflammatory cells evoke neovascularization in the neomembrane of cSDH. Because of these mechanisms, abnormal capillaries were also formed in the same layer.

Observation of sinusoidal capillary in the neomembrane of cSDH was reported in 1975[23,24]. Normally, continuous and fenestrated capillary are found in the dura mater, but sinusoidal capillary is not[22]. Sinusoidal capillary is only found in the liver, bone marrow, spleen, and brain circumventricular organs in normal[22]. It means that the sinusoidal capillary may be newly formed in the condition of cSDH. Capillary is the smallest blood vessel so its characteristic is hard to observe using immunohistochemistry. Therefore, I performed taking TEM which is enough to zoom in on the cell size to confirm the previous results. In this study, sinusoidal

capillaries were observed only in the neomembrane of cSDH dura, not in the DBC layer of control dura.

There are three types of capillaries: continuous, fenestrated, and sinusoidal, these are distinguished by endothelial cell structures. Continuous capillaries have tight junctions between endothelial cells. Fenestrated capillaries have pores with diaphragms between endothelial cells. Sinusoidal capillaries have wide lumen, incomplete basement membrane, lacking smooth muscle cells, and gaps between endothelial cells without junctions[22,23,24]. Based on these features, endothelial cells in the capillaries were observed and classified the capillary types. Continuous capillaries were found in both of the dura mater tissues. However, the fenestrated capillary was only found in the neomembrane of cSDH dura, not in the DBC layer of control dura. Same as previous results, the sinusoidal capillary was observed in the neomembrane layer of cSDH dura. Therefore, this result suggests that those sinusoidal capillaries were newly formed with neovascularization in the neomembrane.

Because of sinusoidal capillary structural features, this type of capillary has been considered weak and fragile[22,24,25]. Also, gaps with no junctions between endothelial cells allow exudation of erythrocytes[24]. Its fragility and leaky can drive the growth of hematoma and have been considered the causation of recurrent cSDH[26]. In addition, counting the capillaries of each type in the tissues was tried. However, the tissue was stored in 10% paraformaldehyde over the two weeks so, most the capillary structures were broken. It was impossible to compare the number of capillaries between each type.

The MMA in the periosteal layer was connected to relatively abundant arteries in the cSDH neomembrane. From the external carotid artery, the maxillary artery branched out then, another branch from the maxillary goes into the skull through the foramen spinosum. This artery is MMA. All small arteries in dura derive from MMA and they connect to each other[27]. αSMA staining of dura tissues showed the connections between MMA and arteries in the

neomembrane. Those arteries in the neomembrane had higher volume density rather than the DBC layer in control. It may indicate the neovascularization of the artery in the cSDH neomembrane.

Newly formed vessels stretched out from pre-existing vessels. Therefore, I assumed that the MMA may connect to newly formed arteries in the neomembrane layer and supply blood. Some non-histological studies were reported the similar results using angiography in cSDH patients[14,27,28]. However, this study is the first histological observation of artery neovascularization.

Inevitably, MMA connects to newly formed vessels including newly formed arteries and sinusoidal capillaries. It means that a high amount of blood might be supplied to newly formed arteries than control. An increase in supplied blood may affect sinusoidal capillaries and evoke rupture of vessels or leakage of blood. Spontaneous resolution implies that the hematoma or blood can be absorbed naturally in the body. However, the overwhelming speed of blood accumulation may disrupt the balance of supplying and draining. It indicates that the connection between MMA and newly formed vessels may be the main cause of hematoma growth or spontaneous recurrent cSDH. This hypothesis supports the micro-hemorrhage from the fragile vessels, also may explain the principle of MMA embolization effectiveness in cSDH patients[32]. (Figure.10) However, the experiment was conducted with a sample from only one cSDH patient. So, it is necessary to research other cSDH cases to generalize this hypothesis.

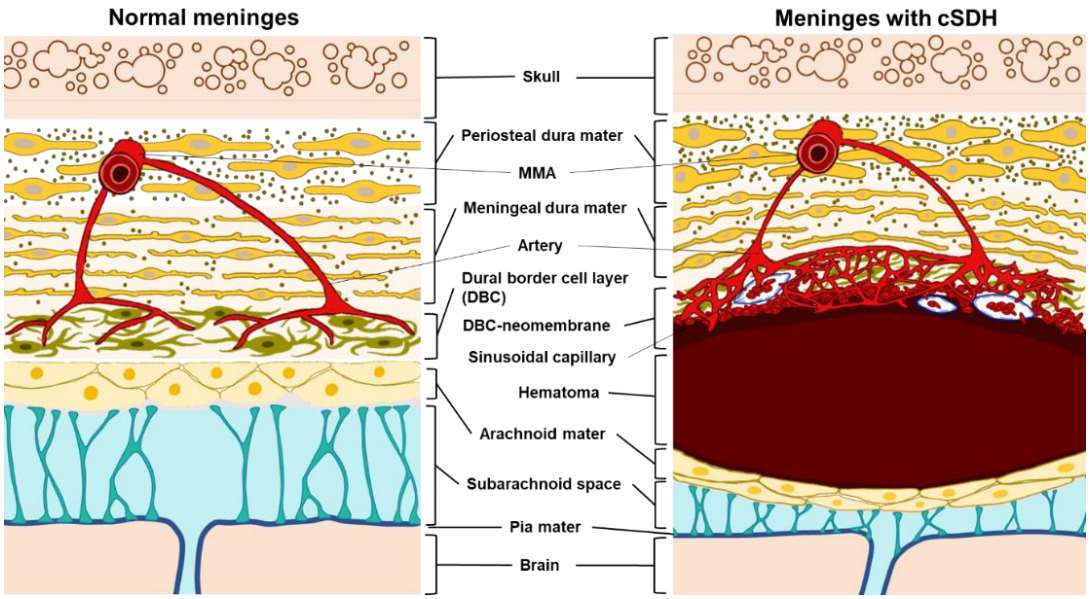

Figure 10. Illustration of normal and cSDH dura mater with vessels.

Compared to the control dura mater, abundant arteries derived from MMA spreads in the neomembrane layer. Also, the sinusoidal capillaries are found in the same layer.

In 1994, MMA embolization was first introduced for the novel treatment of cSDH[15]. Then, Mandai et al. reported the successful treatment of cSDH using MMA embolization in 2000[29]. After MMA embolization was introduced, many cases have shown potential as a new therapy for cSDH for several years[30,31]. The recurrence rate of cSDH after MMA embolization is about 2%. This rate is much lower than conventional surgical removals (2-37%)[30,31]. Also, Ban et al. reported that the treatment failure rate in embolization was only 1.4% but, conventional treatment was 27.5%[30]. These statistical analyses of case reports of MMA embolization in cSDH prove that MMA embolization effectively decreases the rate of recurrence than other surgical removals. Almost 97.8% of patients showed the spontaneous regression of hematoma at 6 months of follow-up[27,30,31,33]. According to the results of this study, the reduction of supplied blood into dura by embolization of MMA is the principle of MMA embolization treatment in cSDH patients. Even though MMA embolized, dura can be supplied blood from other connections. However, MMA is the main bloodstream route so, embolization can effectively regulate the amount of blood. By reducing the continuous accumulation of blood, remained hematoma can spontaneously regress.

Hematoma is absorbed after MMA embolization or spontaneously. The main route of hematoma absorption had been unknown. In 2015, the novel function of lymphatic vessels in meninges was introduced that it drains macromolecules, CSF, and brain interstitial fluid (ISF) to out of the brain[34]. Similarly, meningeal lymphatic vessels also drained erythrocytes out of the brain in SDH and SAH rodent model. These studies confirmed that the drained red blood cells were transferred into deep cervical lymph node (dCLN)[35,36].

As a result of lymphatic vessels in the dura of cSDH patients, lymphatic vessels showed relatively 26.9 times more sprouts and 58.8 times more loops than control dura. In blood vessels, development of sprout and loop structures mean angiogenesis. The formation of tip and stalk cells is induced by growth factors and it becomes sprout form from pre-existing vessels.

Then, two adjacent sprouted endothelial cells form a loop by connecting above the stalk cells during the angiogenesis. Therefore, sprout and loop structure generally indicate angiogenesis[37]. This meaning is as same as in lymphatic vessels. Thus, many articles proved lymphangiogenesis by counting sprouts, loops and calculating area[35,36,38]. However, it was impossible to compare lymphatic vessels in the same regions so, only sprouts and loops were counted without calculating the area. Relatively more sprouts and loops indicate the occurrence of lymphangiogenesis in cSDH patient dura.

The possibility of lymphangiogenesis in cSDH was suggested by Liu et al. They reported that meningeal lymphatic-related markers such as LYVE-1, FOXC 2, and VEGF-C expression were gradually increased in the SDH[35]. Not only in the SDH animal model, but the traumatic brain injury (TBI) animal model also proved lymphangiogenesis in meningeal lymphatics nearby superior sagittal sinus (SSS) and transverse sinus (TS) by immunostaining of meninges[39]. In contrast, lymphangiogenesis-related structures were not detected in any regions of the SAH animal model[36]. I also used SAH patient dura for control, but there were no lymphangiogenesis-related structures such as sprouts and loops same as animal experiments.

Same as neovascularization, lymphangiogenesis is also related to inflammation. VEGF-C released from macrophages in inflammation conditions induces lymphangiogenesis[18,19]. VEGFR3 on the lymphatic endothelial cell surface binds to VEGF-C. This molecular signaling induces DLL4/Notch signaling and then tip/stalk cells are formed on the pre-existing lymphatic vessel[40,41]. Hematoma induces inflammation and recruited macrophages increase the level of VEGF-C in dura[18,19,34,38].

The role of lymphangiogenesis has still not been elucidated but, it is presumed that lymphangiogenesis may enhance the lymphatic drainage function by extended area. Ablation of the part of the lymphatic vessels in meninges showed drainage dysfunction in animal experiments[34,38,42]. On the other hand, VEGF-C injection promoted the drainage of the amyloid-

beta in the Alzheimer's disease mouse model[43]. Also, artificially induced lymphatic dysfunction by ligating dCLN was recovered with increasing lymphatic markers after injecting VEGF-C[35]. Although lymphangiogenesis occurred spontaneously by inflammation, it may recover or enhance meningeal lymphatic drainage function.

In human, meningeal lymphatic vessels are mainly distributed around the dural venous sinus, especially running parallel to the regular venous and straight sinus as similar with mouse[44]. Additionally, as found in rodents, meningeal lymphatic vessels are found around the intrajugular vein and are linked to dCLN[45]. The relationship between meningeal lymphatic vessels and cSDH has not been researched yet in humans. If meningeal lymphatics drain hematoma, its distribution and expansion may help to treat cSDH.

cSDH has no standard to predict patient prognosis so, the brain is periodically followed up by magnetic resonance imaging (MRI), and computed tomography (CT) until hematoma disappears. In some cases of SDH, hematoma in the parietal region relatively showed high occurrence rate with low spontaneous resolution than the other regions[47]. On the other hand, there was a report that only 5 patients among 24 patients showed spontaneous resolution of hematoma in the fronto-parietal region[48]. These reports suggest the possibility that the spontaneous resolution of hematoma may relate to the region. So, I expect that meningeal lymphatic distribution around the hematoma region may affect the resolution of hematoma and this can be a standard for predicting the patient prognosis. So far, people have studied the waste clearance pathway by imaging glymphatic-lymphatic system using MRI, CT, and positron emission tomography (PET)[44,45,46]. Therefore, lymphatic system imaging of SDH patients may need to study for the new standard.

Moreover, enhancement of hematoma drainage by inducing lymphangiogenesis may help to treat cSDH in another way. Lymphangiogenesis is usually considered to enhancing the drainage function by extending its area. Like previous animal studies, induced lymphangiogenesis of

meningeal lymphatics can promote drainage function and it may accelerate the absorption of hematoma in humans. However, the patient needed surgical removal even though lymphangiogenesis was observed in the dura. It means that it is also necessary to prove that the newly formed sprouts and loops enhance the drainage function. Even if MMA embolization effectively reduces the blood supplying and blocks the re-growth of hematoma, existing hematoma needs to remove or absorb. Therefore, developing spontaneous resolution of hematoma by studying meningeal lymphatics can be suggested a novel treatment for cSDH patients.

Conclusion

In conclusion, histopathological changes of vasculature in spontaneous recurrent cSDH were comprehensively evaluated. The increase of vessel density including arteries and, formation of the sinusoidal capillary in the neomembrane, and abundant lymphatic sprouts and loops were observed in the cSDH dura mater, suggesting neovascularization. Furthermore, the MMA in the periosteal layer was connected to relatively abundant arteries in the cSDH neomembrane. These results can support the main hypothesis of spontaneous recurrent cSDH and explain the therapeutic mechanism of MMA embolization.

References

1. Yang W, Huang J. Chronic subdural hematoma epidemiology and natural history. *Neurosurgery Clinics North America*. 2017;28:205-10.

2. Rauhala M, Luoto T, Huhtala H, Iverson G, Niskakangas T, et al. The incidence of chronic subdural hematomas from 1990-2015 in a defined Finnish population. *Journal of Neurosurgery*. 2019;22:1-11.

3. Yadav Y, Parihar V, Namdev H, Bajaj J. Chronic Subdural Hematoma. *Asian Journal of Neurosurgery*. 2016;11(4):330-42.

4. Adeeb N, Mortazavi M, Tubbs R, Cohen-Godol A. The cranial dura mater: a review of its history, embryology, and anatomy. *Childs Nervous System*. 2012;28:827-837.

5. Lee KS. Natural history of chronic subdural hematoma. *Brain Injury*. 2004;18(4):351-8.

6. Cho WS, Batchullun Batbold, Lee SJ, Kang HS, Kim JE. Recurrent subdural hematoma from a pseudoaneurysm at the cortical branch of the middle cerebral artery after mild head injury. *Neurologica medico-chirurgica (Tokyo).* 2011;51:217-21.

7. Rambaud C. Bridging veins and autopsy findings in abusive head trauma. *Pediatric Radiology*. 2015;45:1126-31.

8. Beck J, Gralla J, Fung C, et al. Spinal cerebrospinal fluid leak as the cause of chronic subdural hematomas in nongeriatric patients. *Journal of Neurosurgery.* 2014;121:1380-7.

9. Yang AI, Balser DS, Mikheev A, et al. Cerebral atrophy is associated with development of chronic subdural haematoma. *Brain Injury*. 2012;26:1731-6.

10. Kim HC, Ko J, Yoo D, Lee S. Spontaneous resolution of chronic subdural hematoma: close observation as a treatment strategy. *Journal of Korean Neurosurgical Society*. 2016;59(6):628-36.

11. Almenawer SA, Farrokhyar F, Hong C, et al. Chronic subdural hematoma management: a systematic review and meta-analysis of 34,829 patients. *Annals of Surgery.* 2014;259:449-57.

12. Weigel R, Hohenstein A, Schlickum L, Weiss C, Schilling L. Angiotensin converting enzyme inhibition for arterial hypertension reduces the risk of recurrence in patients with chronic subdural hematoma possibly by an antiangiogenic mechanism. *Neurosurgery.* 2007;61:788-92.

13. Hirashima Y, Kurimoto M, Nagai S, Hori E, Origasa H, Endo S. Effect of platelet-activating factor receptor antagonist, etizolam, on resolution of chronic subdural hematoma--a prospective study to investigate use as conservative therapy. *Neurologica medico-chirurgica (Tokyo).* 2005;45:621-6.

14. Gernsback J, Kolcun J, Jagid J. To drain or two drains: Recurrences in chronic subdural hematomas. *World Neurosurgery*. 2016;95:447-50.

15. Komiyama M, Yasui T, Tamura K, Nagata Y, Fu Y, Yagura H. Chronic subdural hematoma associated with middle meningeal arteriovenous fistula treated by a combination of embolization and burr hole drainage. *Surgical Neurology*. 1994;42:316–9.

16. Petrova T, Koh G. Biological functions of lymphatic vessels. *Science.* 2020;369:eaax4063.

17. Sahyouni R, Goshtasbi K, Mahmoodi A, Tran D, Chen J. Chronic subdural hematoma: a perspective on subdural membranes and dementia. *Word Neurosurgery*. 2017;108:954-8.

18. Edlmann E, Giorgi-Coll S, Whitfield P, Carpenter K, Hutchinson P. Pathophysiology of chronic subdural haematoma: inflammation, angiogenesis and implications for pharmacotherapy. *Journal of Neuroinflammation*. 2017;14:108-22.

19. Shono T, Inamura T, Morioka T, et al. Vascular endothelial growth factor in chronic subdural haematomas. *Journal of Clinical Neuroscience.* 2001;8:411-5.

20. Stanisic M, Aasen AO, Pripp AH, et al. Local and systemic pro-inflammatory and anti-inflammatory cytokine patterns in patients with chronic subdural hematoma: a prospective study. *Inflammation Research.* 2012;61:845-52.

21. Koh BI, Lee HJ, Kwak PA, Yang MJ, Kim JH, et al. VEGFR2 signaling drives meningeal vascular regeneration upon head injury. *Nature communications*. 2020;11:3866.

22. Augustin H, Koh G. Organotypic vasculature: From descriptive heterogeneity to functional pathophysiology. *Science*. 2017;357:eaal2379.

23. Sato S, Suzuki J. Ultrastructural observations of the capsule of chronic subdural hematoma in various clinical stages. *Journal of Neurosurgery*. 1975;43:569-78.

24. Yamashima T, Yamamoto S, Friede RL. The role of endothelial gap junctions in the enlargement of chronic subdural hematomas. *Journal of Neurosurgery* 1983;59:298-303.

25. Moskala M, Goscinski I, Kaluza J, et al. Morphological aspects of the traumatic chronic subdural hematoma capsule: SEM studies. *Microscopy and Microanalysis.* 2007;13:211-9.

26. Shim Y, Park C, Hyun D, Park H, Yoon S. What are the causative factors for capillary a slow, progressive enlargement of a chronic subdural hematoma? *Yonsei Medical Journal*. 2007;48:210-7.

27. Moshayedi Pouria, S. Liebeskind David. Middle meningeal artery embolization in chronic subdural hematoma: Implications of pathophysiology in Trial design. *Frontiers in Neurology*. 2020;11:923-9.

28. Saito Hiroshi, Tanaka Michihiro, Hadeishi Hiromu. Angiogenesis in the septum and inner membrane of refractory chronic subdural hematomas: Consideration of findings after middle meningeal artery embolization with low-concentration n-butyl-2-cyanoacrylate. *NMC Case Report Journal.* 2019;6:105-110.

29. Mandai S, Sakurai M, Matsumoto Y. Middle meningeal artery embolization for refractory chronic subdural hematoma. *Journal of Neurosurgery*. 2000;93:686-8.

30. Ban SP, Hwang G, Byoun H, Kim T, Lee S, et al. Middle meningeal artery embolization for chronic subdural hematoma. *Neuroradiology*. 2018;286:992-9.

31. Link T, Boddu S, Paine S, Kamel H, Knopman J. Middle Meningeal artery embolization for chronic subdural hematoma: A series of 60 cases. *Neurosurgery*. 2019;85:801-7.

32. Martinez-Perez R, Rayo N, Tsimpas A. Endovascular embolization of the middle meningeal artery to treat chronic subdural haematomas: effectiveness, safety, and the current controversy. A systematic review. *Neurologia*. 2020; 2173-5808.

33. Shapiro Maksim, Walker Melanie, Carroll Kate T, Levitt Michael R, Raz Eytan, et al. Neuroanatomy of cranial dural vessels: implications for subdural hematoma embolization. *Journal of NeuroInterventional Surgery.* 2021;0:1-8.

34. Louveau Antoine, Smirnov Igor, Keyes Timothy J, Eccles Jacob D, Rouhani Sherin J, et al. Structural and functional features of central nervous system lymphatics. *Nature.* 2015;523(7560):336-41.

35. Liu X, Gao C, Yuan J, Xiang T, Gong Z, et al. Subdural haematomas drain into the extracranial lymphatic system through the meningeal lymphatic vessels. *Acta Neuropathologica Communications*. 2020;8:16-27.

36. Chen J, Wang L, Xu H, Xing L, Zhuang Z, et al. Meningeal lymphatics clear erythrocytes that arise from subarachnoid hemorrhage. *Nature communications.* 2020;11:3159-3174.

37. Uccelli A, Wolff T, Valenta P, Maggio N, Pellegrino M, et al. Vascular endothelial growth factor biology for regenerative angiogenesis. *Swiss Medical Weekly*. 2019;149:w20011.

38. Louveau Antoine, Herz Jasmin, Alme Nordheim Maria, Salvador Andrea Francesca, Q. Dong Michael, et al. CNS lymphatic drainage and neuroinflammation are regulated by meningeal lymphatic vasculature. *Nature Neuroscience*. 2018;21:1380-91.

39. Bolte A, Dutta A, Hurt M, Smirnov I, Kovacs M, et al. Meningeal lymphatic dysfunction exacerbates traumatic brain injury pathogenesis. *Nature communications*. 2020;11:4524-42.

40. Jakobsson Lars, Franco Claudio A, Bentley Katie, Collins Russell T, Ponsioen Bas, et al. Endothelial cells dynamically compete for the tip cell position during angiogenic sprouting. *Nature Cell biology*. 2010;12:943-69.

41. Zheng Wei, Tammela Tuomas, Yamamoto Masahiro, Anisimov Andrey, Holopainen Tanja, et al. Notch restricts lymphatic vessel sprouting induced by vascular endothelial growth factor. *Blood*. 2011;118:1154-62.

42. Christensen J, Wright D, Yamakawa G, Shultz S, Mychasiuk R. Repetitive mild traumatic brain injury alters glymphatic clearance rates in limbic structures of adolescent female rats. *Scientific Reports*. 2020;10:6254-63.

43. Wen Y, Yang J, Wang X, Yao Z. Induced dural lymphangiogenesis facilities soluble amyloid-beta clearance from brain in a transgenic mouse model of Alzheimer's disease. *Neural Regeneration Research*. 2018;13:709-16

44. Abstina Martina, Ha SK, Nair G, Sati P, Luciano NJ, et al. Human and nonhuman primate meninges harbor lymphatic vessels that can be visualized noninvasively by MRI. *eLife*. 2017;6:e29738.

45. Yamurlu K, Sokolowski JD, Cirak Musa, Urgun K, Soldozy S, et al. Anatomical features of the deep cervical lymphatic system and intrajugular lymphatic vessels in human. *Brain Sciences*. 2020;10:953-65.

46. Iliff Jeffery J, Lee HD, Yu Mei, Feng Tian, Jean Locan, et al. Brain-wide pathway for waste clearance captured by contrast-enhanced MRI. *Journal of Clinical Investigation*. 2013;123:1299-1309.

47. Son S, Yoo CJ, Lee SG, Kim EY, Park CW, et al. Natural course of initially non-operated cases of acute subdural hematoma: The risk factors of hematoma progression. *Journal of Korean Neurosurgical Society*. 2013;54:211-219.

48. Parlato Ciro, Guarracino Antonino, Moraci Aldo. Spontaneous resolution of chronic subdural hematoma. *Surgical Neurology*. 2000;53:312-317.

요약(국문초록)

재발한 만성 경막하 혈종에서 혈관 구조 변화의 조직 병리학적 평가

김 현

분자의학 및 바이오제약학과

서울대학교 융합과학기술대학원

만성 경막하 혈종은 뇌경막하 공간에 출혈이 축적되어 혈종이 생기고 이 혈종이 신생막으로 감싸져 있는 질환을 의미한다. 이 질환의 발생률은 노년층을 중심으로 매년 증가하고 있는 추세이다. 혈종 제거 수술 후에도 해당 질환이 재발하는 비율이 상당히 높다. 여전히 자연적으로 질환이 재발되는 원리는 밝혀지지 않고 있으며, 이에 대한 표준 치료법이 확립되어 있지 않다. 만성 경막하 혈종의 자연적 재발에서 밝혀지지 않은 문제들을 풀기 위해, 혈관 구조의 변화들을 중심으로 만성 경막하 혈종 환자의 경막을 조직 병리학적으로 관찰하였다.

환자들로부터 얻은 정상 경막과 만성 경막하 혈종의 경막을 서로 비교하였다. 해당 연구에서는 주로 면역 염색 기법이 관 구조들을 시각화 하는데 이용되었으며, 3 차원 구조로 경막의 모든 층을 관찰하기 위해서 조직 투명화 기법도 이용하였다. 추가적으로, 투과전자현미경(TEM)은 모세혈관들과 해당 내피 세포들을 관찰하는 데 사용되었다.

실험 결과, 만성 경막하 혈종 환자의 속판(meningeal dura)은 정상 경막에 비해서 얇았다. 반대로, 경막 경계 세포 층은 환자의 경우 신생막으로 변화하기 때문에 더 두껍게 관찰되었다. 환자의 신생막 층에서, 혈관이 차지하는 부피는 정상적인 경막의 경계 세포 층에 있는 혈관의 부피에 비해서 5.9 배 밀도가 더 높은 것을 확인했다. 그리고 sinusoidal 모세혈관 (sinusoidal capillary)이 신생막 층에서 형성된 것을 TEM 을 이용해 관찰하였다. 또한, 환자의 신생막 층에서 정상적인 경막의 경계 세포 층에 비해 5.4 배 높은 밀도의 동맥이 발견되었다. 해당 동맥들은 중간뇌막동맥과 연결되어 있음을 확인했다. 추가적으로, sprout 와 loop 구조의 형성을 통해서 림프관의 구조적 변화가 발생했음을 관찰했다. 정상에 비해서 조직의 부피 당, 26.9 배 더 많은 sprout 와 58.8 배 더 많은 loop 구조가 형성되어 있었다.

따라서, 환자의 신생막 층에서는 혈관 밀도의 증가와 약하고 잘 새는 구조의 모세혈관이 관찰되었고, 이는 만성 경막하 혈종 발생 시, 경막에서 신생혈관이 형성됨을 의미한다. 특히, 중간뇌막동맥과 신생막에서 밀도가 높은 동맥간 연결성이 조직학적으로 확인되었다. 이는 아마도 만성 경막하 혈종이 재발하는 원인에 대한 가설을 뒷받침하고, 더 나아가 중간뇌막동맥 색전술을 이용한 치료법의 효과 원리를 설명할 수 있을 것이다.

주요어: 만성 뇌경막하 혈종, 뇌경막, sinusoidal 모세혈관 구조, 중간뇌막동맥, 신생 혈관 형성, 신생 림프관 형성

학 번: 2019-28947